

Massively Parallel Open Modification Spectral Library Searching with Hyperdimensional Computing

Jaeyoung Kang, Weihong Xu, Wout Bittremieux, Tajana Rosing

University of California, San Diego

{j5kang, wexu, wbitremieux, tajana}@ucsd.edu

ABSTRACT

Mass spectrometry, commonly used for protein identification, generates a massive number of spectra that need to be matched against a large database. In reality, most of them remain unidentified or mismatched due to unexpected post-translational modifications. Open modification search (OMS) has been proposed as a strategy to improve the identification rate by considering every possible change in spectra, but it expands the search space exponentially. In this work, we propose HyperOMS, which redesigns OMS based on hyperdimensional computing to cope with such challenges. Unlike existing algorithms that represent spectral data with floating point numbers, HyperOMS encodes them with *high dimensional binary vectors* and performs the efficient OMS in high-dimensional space. With the massive parallelism and simple boolean operations, HyperOMS can be efficiently handled on parallel computing platforms. Experimental results show that HyperOMS on GPU is up to 17× faster and 6.4× more energy efficient than the state-of-the-art GPU-based OMS tool [9] while providing comparable search quality to competing search tools.

CCS CONCEPTS

- Computing methodologies → Massively parallel algorithms; • Applied computing → Computational proteomics.

KEYWORDS

Spectral library search, Mass spectrometry, Proteomics, Hyperdimensional computing

1 INTRODUCTION

Proteomics plays an essential role in understanding the molecular mechanisms of proteins, which are responsible for various tasks in a life of a cell [4]. Mass spectrometry (MS) is one of the most popular and reliable approaches to identifying and quantifying proteins and peptides in complex biological samples [40]. In a typical MS experiment, a method called tandem mass spectrometry (MS/MS) generates a massive amount of MS/MS spectra data. Then researchers determine peptide annotations of the MS/MS spectra via spectral library searching [28]. Peptide sequences are assigned to experimental MS/MS spectra by matching them against a spectral library of known peptides (see Figure 1).

The challenge of spectral library searching is that a significant portion of MS/MS spectra acquired during an experiment cannot be directly identified [12] using searching approaches with conventional similarities, such as cosine similarity. In reality, proteins undergo one or more post-translational modifications (PTMs), which change their mass and MS/MS fragmentation pattern. PTMs can be introduced during sample preparation as an artifact of MS measurement [8], or biologically relevant PTMs arise *in vivo* [41]. However,

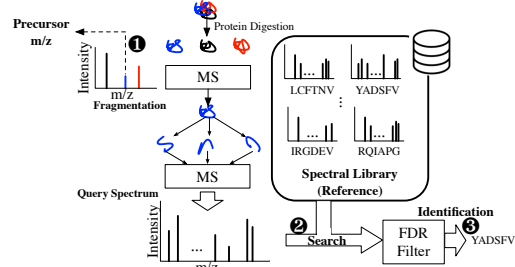


Figure 1: Overview of spectral library searching. Standard searching uses a narrow precursor m/z tolerance, while OMS uses a wide precursor m/z tolerance during the searching.

spectral libraries mainly contain reference spectra for unmodified peptides, so PTMs make experimental spectra challenging to identify as they no longer exactly match the reference spectra.

Open modification searching (OMS) is a promising approach to circumvent this limitation and identify modified spectra [33]. Standard spectral library searching only compares experimental spectra to reference spectra with a similar precursor mass, i.e., the mass of the unfragmented peptide, as matching peptides should have an identical mass. In contrast, OMS performs spectra matching on a wider range of reference spectra, where OMS compares modified query spectra to their unmodified reference variants, even when their precursor mass differs due to PTMs. OMS' wider searching range empowers higher identification capability, thus enabling the study of more complex protein interaction in virus-host [3] and proteomics analysis of non-model organisms [17].

OMS faces several challenges in terms of low searching speed, efficiency, and accuracy. Compared to standard searching, the OMS speed is extremely slow due to the drastically increased search space since it considers all possible reference matches for each query spectrum [7]. This problem is further exacerbated by the increasing spectral data due to the cost reduction in the MS experiment (2× in recent two years) [5, 35]. Also, large spectral libraries created by repository-scale mining of open MS data become available [16, 42]. For example, the size of human HCD (higher energy collisional dissociation) spectral libraries [1, 42] hold 2.15 million data points, which is 4× larger than the previous NIST-HCD [42]. MassIVE contains 5.6 billion spectra, which corresponds to 448TB in size [2].

Several tools have been introduced to efficiently perform OMS [7, 9, 11, 13, 27, 29, 32]. These tools use various techniques to refine the search space, such as fragment ion indexing [27], nearest neighbor searching [7, 9], or tag-based filtering [11, 13]. For example, the state-of-the-art OMS tool ANN-SoLo performs nearest neighbor searching using GPU and computes shifted cosine similarities on candidates [9]. However, existing solutions involve a complex

execution pipeline and exhibit low data parallelism requiring high-precision floating-point (FP32) arithmetic for good search quality, e.g., shifted cosine similarity [7]. As such, we redesign an OMS algorithm that only involves hardware-friendly Boolean operations with a simple execution pipeline.

In this work, we propose novel hyperdimensional computing (HDC)-inspired OMS algorithm called HyperOMS. The spectral matching algorithm of HyperOMS is based on the efficient computing paradigm, HDC [21], that has shown high efficiency for pattern matching tasks, especially on parallel computing platforms, e.g., GPU [22, 23]. HDC improves the data separability and robustness [36, 44] by mapping data into high-dimensional (HD) space, where the information is distributed to every dimension of the HD vector. We leverage HDC’s robustness to minimize the effects of PTMs. In particular, our method reflects the spatial and value locality of peaks in the spectrum, making the encoded data resilient to peak shifts and intensity changes. HyperOMS addresses the search space challenges in OMS by approximating possible MS peak changes; spectra can be identified with a single similarity computation. Furthermore, the proposed HDC-empowered OMS algorithm is hardware-friendly as it replaces FP32 operations with simple Boolean arithmetic by encoding data into binary HVs, leading to better computational efficiency. We implement the HyperOMS algorithm on the high-performance HDC library [22, 23] on GPU, obtaining up to 17 \times speedup and 6.4 \times energy efficiency over the state-of-the-art OMS solution, ANN-SoLo [9] while offering comparable search quality.

2 BACKGROUND AND RELATED WORK

2.1 Mass Spectrometry Background

MS is used to study the biological process in proteomics via the analysis of protein expression or state in cells or tissue [40]. Proteins are ubiquitous building blocks of life, and they are composed of peptides, which are chains of amino acids, which can be described as a string of letters.

During MS data acquisition, peptides are ionized to receive a charge, and their mass-over-charge (m/z) is measured. The first intact ions are measured in an MS scan using data-dependent acquisition, and the resulting MS spectrum contains the corresponding m/z values. The most intense peaks in the MS spectrum are selected. It is further analyzed in MS/MS scans, i.e., the second mass spectrometer. Ions with matching m/z are isolated and fragmented to generate MS/MS spectra. Fragmentation occurs along the peptide backbone in between its constituent amino acids. Peptides are split into their possible amino acid subsequences. We record the m/z and intensity values of all fragments, and the measured spectrum forms a *unique fingerprint of the measured peptide*. Thus, each MS/MS spectrum consists of fragment m/z values, *spectrum charge*, and its intact m/z from the preceding MS scan, called the *precursor m/z* (Figure 1-❶).

Spectral library searching determines which peptide corresponds to the measured spectra [28]. (Figure 1-❷). A spectral library contains reference spectra, each with known peptide labels. We first select the reference candidates with a similar precursor m/z to a query spectrum. Next, similarities between the query spectrum and all candidates are computed. Finally, the query spectrum is assigned the same peptide label as its highest-scoring reference match. Here,

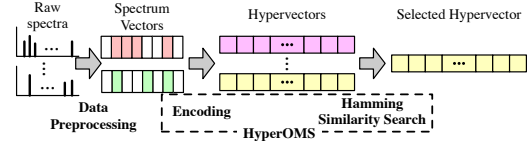


Figure 2: Overview of OMS process using HyperOMS.

we apply a false discovery rate (FDR) filter on search results [14] (Figure 1-❸), which is a popular strategy called target-decoy strategy [14] in MS/MS analysis to reduce false positives. Decoy spectra that cannot exist are added to the spectral library besides the real (target) spectra. Decoy spectra selected by the searching tool are filtered out. The number of target SSMs and decoy SSMs at a specific score can be used to compute the FDR. Typically, an FDR threshold of 1% is used to minimize the number of incorrect identifications. The performance of different search tools can be compared by *the number of identified spectra* at a fixed FDR threshold.

A **standard searching** strategy can identify directly matching spectra. It assumes that precursor m/z of query and matched reference spectra are similar (narrow precursor m/z tolerance). However, as spectral libraries mainly contain unmodified reference spectra, they cannot be used to identify modified ones. Modified ones have a different intact mass, as the modifications induce mass shifts. **Open modification searching (OMS)** addresses these issues by (i) using a wide precursor m/z tolerance that exceeds mass shifts induced by modifications to select reference candidates [33], and (ii) using alternative spectrum similarity measures that take peak shifts due to modifications into account [7]. Using a wide precursor m/z tolerance enables finding (partial) matches between unmodified reference spectra and their modified variants. However, a large number of candidates need to be evaluated for each query spectrum, which can be computationally demanding.

2.2 Accelerated Spectral Library Searching

OMS has recently become an increasingly popular search strategy, and there have been several studies to accelerate searches on different hardware platforms. On CPU, MSFragger [27] uses a fragment ion index to retrieve matching reference spectra. ANN-SoLo [7, 9] is a state-of-the-art OMS tool that uses GPU-powered nearest neighbor searching library, Faiss [20], to prune the search space. Several studies have focused on accelerating spectral library searching using GPUs for efficient spectrum–spectrum similarity computation [6, 31]. [43] used a CPU-FPGA architecture in which multiple FPGAs are used for scalability and parallelism. However, none of these studies have addressed the OMS challenges.

3 HYPEROMS ALGORITHM

HyperOMS encodes raw spectral data to a binary HD vector called *hypervector* (HV) to capture the position and intensities of peaks while considering the spatial locality and value locality. Although peaks are shifted due to PTMs, the similarity between a query spectrum and a matching reference spectrum does not change dramatically. Furthermore, since binary vector representation is used, HyperOMS replaces complex similarity metrics in existing OMS tools with a simple Hamming similarity operation.

3.1 Overall Flow

Figure 2 shows a flow of HyperOMS. It starts with a data preprocessing step, a common step for OMS. It refines and vectorizes raw

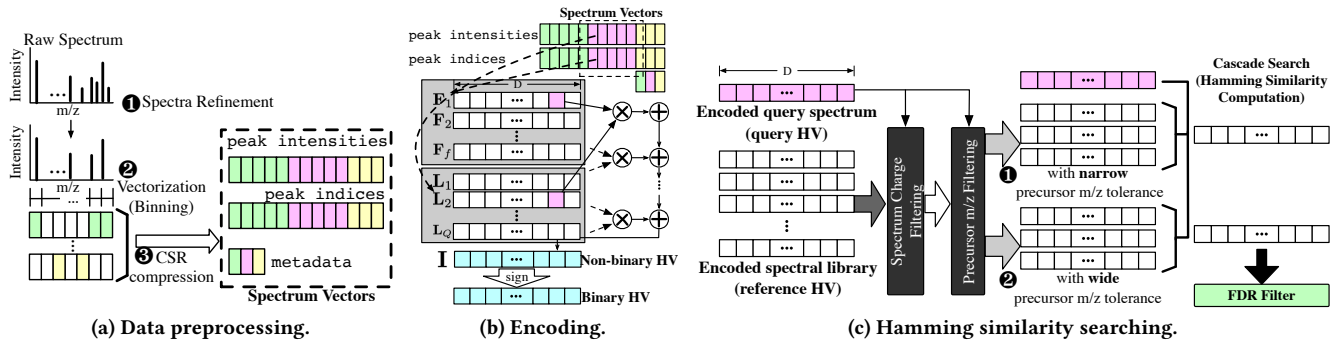


Figure 3: Data preprocessing and stages of HyperOMS algorithm.

spectra and compresses them, resulting in spectrum vectors. HyperOMS encodes spectrum vectors into HV during the encoding step. Next, the Hamming similarity searching step filters reference spectra according to the query’s precursor m/z and spectrum charge and computes Hamming similarity between query HVs and candidate reference HVs.

3.2 Data Preprocessing

The preprocessing step (1) refines the raw spectra by removing redundant peaks and (2) vectorizes refined spectra (see Figure 3(a)). First, raw spectra are refined to gather meaningful peaks (1). We remove peaks whose intensity is below 1% of the most intense peaks. Low-intensity peaks are considered noise. In turn, we retain 50 to 150 most intensive peaks of the spectra. Existing studies [9, 29] have shown that we can effectively refine spectra in this manner.

Next, we vectorize the filtered spectra (2). The peaks are discretized by binning the m/z range to represent a spectrum into a sparse vector of floating-point intensity values, called a *spectrum vector*. If multiple peaks are assigned to the same m/z bin, we sum their intensity values. A large bin width can lead to loss of information when peaks are grouped into a single bin. For example, the mass range between 0 m/z and 2000 m/z and bin width 0.04 (based on the resolution of the mass spectrometer) results in a dimensionality of 50,000. The resulting spectrum vectors have sparsity less than 1%. There are 50 to 150 peaks for each spectrum vector, and its dimensionality is 20,000 to 50,000. As such, we compress spectrum vectors in a compressed sparse row (CSR) format (3). The preprocessing step is normally run offline, and the resulting data is stored as a binary file for future use. In the following, we discuss the HyperOMS algorithm, which first encodes spectrum vector to HV and performs searching on HV.

3.3 Encoding: Spectrum Vectors to Hypervectors

HyperOMS encodes the data into a *binary vector representation*, which can enhance the computation efficiency. There have been several efforts to represent raw data in an HD binary vector, using Locality Sensitive Hashing (LSH) [19, 26, 34] or HDC [18, 19, 25, 37]. However, these strategies do not reflect the characteristics of OMS, including peak shifts and intensity changes. For example, they treat each feature position (corresponding to peak indices in spectrum vector) as orthogonal. Peak shifts can lead to significant changes in similarity. Conversely, our encoding takes both *spatial locality* (for peak shift) and *value locality* (for peak intensity change from

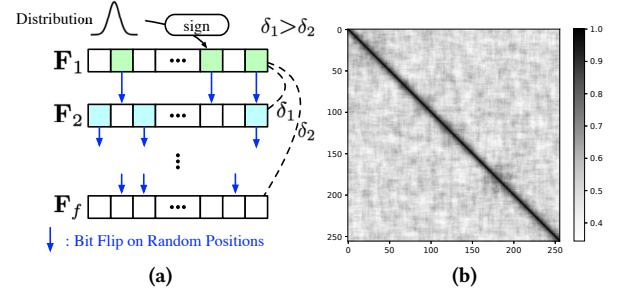


Figure 4: Position HV generation. (a) Strategy overview. (b) Pairwise similarity (Hamming similarity normalized by the HV dimension size) between position HVs.

instrument error or noise) of each feature into account. As a result, we can preserve similarity despite peak changes, which is essential for OMS.

Figure 3(b) shows the encoding process of HyperOMS. Unique *position HVs* F are assigned for each index in a spectrum vector, i.e., F_i corresponds to index i , and $F \in \{F_1, F_2, \dots, F_f\}$. Note that f is the dimensionality of spectrum vector. Similarly, we use *level HVs* L to capture different intensity values in each index. We quantize intensity range into Q levels, and L_i is assigned to each quantization level i where $i \in [0, Q]$. Given two sets of HVs, F and L , a spectrum vector is encoded into a HV I as follows. Let P be the set of peaks in the spectrum vector, consisting of tuples (i, j) , with i the peak index and j the step value of its intensity. I is computed as follows:

$$I = \sum_{(i,j) \in P} F_i \odot L_j, \quad (1)$$

where \odot indicates element-wise multiplication. In turn, we binarize the I for the computational efficiency on hardware; all positive elements are mapped to 1 and -1 otherwise. The final representation of the HV is a binary vector. Spectrum vectors corresponding to the query and reference spectra are encoded to query HVs and reference HVs, respectively. Encoding of reference spectra is done only once. The reference HVs is reused for subsequent runs since they are already identified and unlikely to change.

3.3.1 Reflecting Spatial Locality. We devise the new position HV generation method to reflect the spatial locality. Previous studies [37, 38] have used a permutation-based or random generation

method, which makes F_i and F_j ($i \neq j$) nearly orthogonal. However, they are vulnerable to peak shifts as they accompany changes in i .

Figure 4(a) shows the proposed position HV generation strategy. We randomly generate $F_1 = \{+1, -1\}^D$. In turn, we flip α components in random positions. As more flips occur, the similarity between the original vector and the flipped vector decreases. For example, the similarity (δ_1) between F_1 and F_2 is larger than the similarity (δ_2) between F_1 and F_f . The HyperOMS encoding reflects the characteristics of peak shifts in OMS well: (1) neighboring positions should have spatial locality to deal with peak shifts, while (2) distant positions need to have adequate orthogonality. The peak shift changes the index value corresponding to the intensity in the spectrum vector. Position HVs do not change significantly even if peak shifts occur; the resulting representation can be tolerable to PTMs. As depicted in Figure 4(b), for F_i and F_j , the pairwise similarity has a high value when $i \approx j$ and is maximum when $i = j$ (diagonal elements). Note that we scaled down the f to 128 and D to 256 for better visibility.

3.3.2 Reflecting Value Locality. The intensity information of the spectrum vectors is captured. We use the level HV generation method from [18, 25, 37]. We allocate a single bit to each of the HV components, i.e., $L_i \in \{-1, 1\}^D$. L that is assigned to each quantization level needs to reflect the closeness of the intensity, i.e., value locality. The similarity between L_i and L_{i+1} is higher than the similarity between L_i and L_{i+100} . For instance, for the target level p in percentage, L_p , we can represent this by flipping $(D/2) \times (p/100)$ elements of L_0 .

3.4 Hamming Similarity Search

After the encoding step, HyperOMS finds the matched reference HV that is most similar to the query HV. It uses *Hamming similarity* (defined by the number of equal components in vector pairs) as a similarity metric. Here, reference spectra that need to be compared primarily need to satisfy spectrum charge and precursor m/z condition per query as discussed in Section 2.1. Each spectrum has its spectrum charge ($+2, +3, \dots$) and precursor m/z value. We gather reference spectra that (1) have the same spectrum charge as the query spectra and (2) satisfy the precursor m/z tolerance (precursor m/z difference between query and reference) condition.

OMS assumes that precursor m/z of selected reference spectra and query spectra can have a large difference. In other words, a wide precursor m/z tolerance is used to match modified spectra to their unmodified variants. However, we may miss the case of a reference spectrum with a similar precursor m/z that can pass through the FDR filter with high similarity. To avoid such misidentifications, we adopt *cascade search* [24]. A narrow precursor m/z tolerance is used for standard search and FDR filtration is applied (Figure 3(c)-❶). In turn, remaining unidentified spectra are processed with a wide precursor m/z tolerance (Figure 3(c)-❷).

4 EVALUATION

4.1 Methodology

The evaluation was performed on a system equipped with Intel i7-8700K with 64GB RAM and NVIDIA Geforce GTX 1080Ti. We have implemented the HyperOMS algorithm on GPU based on [22, 23]. To maximize the computation efficiency, we represent binary HV

Table 1: Spectrum preprocessing settings.

Parameter Name	Dataset	
	Small scale	Large scale
Max peaks in spectra	50	
Min / max m/z	101 / 1500	
Bin size	0.05	0.04
Precursor m/z tolerance (narrow)	20ppm	5ppm
Precursor m/z tolerance (wide)	500Da	500Da

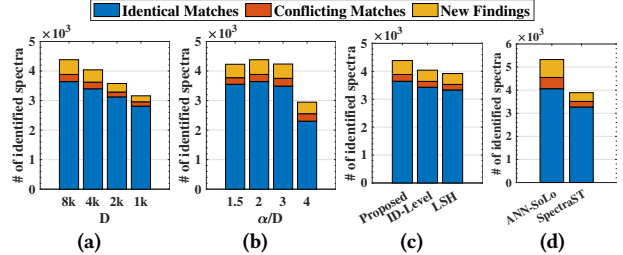


Figure 5: Search quality comparison on the small scale dataset. (a) HyperOMS with different HV dimensionality. (b) HyperOMS with different number of bit flips. (c) HyperOMS with various encoding strategies. (d) Results of baseline tools.

as a 32bit integer array using bit packing, and similarity score computation is done by CUDA intrinsic (`_popc`). Since the GPU has limited memory, we split the reference and the query data into batches. We set the batch size to use the maximum amount of VRAM for GPU-based solutions. We measured the energy consumption of the CPU and GPU using Intel Power Gadget and `nvidia-smi`, respectively.

Workloads. We evaluated HyperOMS on two real-world datasets. Small scale dataset combines yeast spectral library [39] with the human HCD spectral library (total spectra: 1, 162, 392) as the reference libraries, and the iPRG2012 dataset [10] (total spectra: 15, 867) as a query. For a larger-scale evaluation, we used the human spectral library [1, 42] (total spectra: 2, 992, 672) and a HEK293 (Human Embryonic Kidney 293) dataset [12] (total spectra per query: 46, 665 on average), as reference and query spectra, respectively. Note that HEK293 consists of multiple query files (b1906~b1938).

We preprocessed query and reference spectra in a similar fashion to existing works [7, 9, 29], using the widely used configurations listed in Table 1. We removed the duplicates and added decoy spectra with the same ratio as the existing spectral libraries using the shuffle-and-reposition method [30] for FDR filtering.

Benchmarks. We compare the search quality of HyperOMS to existing search tools, including (1) SpectraST [29, 32] that run on CPU and (2) the state-of-the-art OMS tool, ANN-SoLo, running on CPU [7] and GPU [9]. We count the number of identifications to compare the search quality. All search results are evaluated at fixed 1% FDR threshold, using Pyteomics [15].

4.2 Impact of Encoding Configuration

HV dimensionality. The HV dimensionality (D) plays a critical role in search quality. A low D limits separability. Figure 5(a) describes the impact of D . The higher D leads to a higher number of identifications. However, the excessive D leads to an increase in computation and capacity demand. We set the D to 8192 (8k).

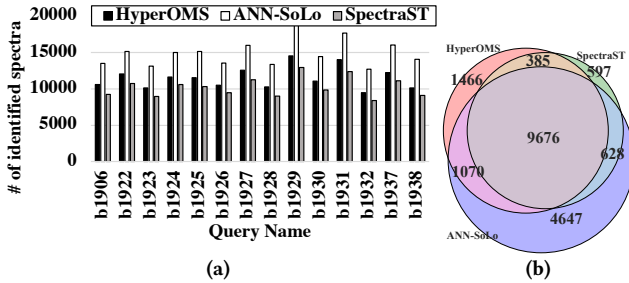


Figure 6: Search result analysis from HyperOMS and baseline tools on the large scale dataset. (a) Total number of identifications. (b) Venn diagram of b1927 query search result.

Flipped bits. The number of flipped bits (α) controls the balance between orthogonality and correlation between bins. A high α increases the orthogonality of each position, and a low α helps a more number of adjacent bins to have a correlation (spatial locality). We measured the number of identifications according to the ratio of flips to D , i.e., α/D . As shown in Figure 5(b), an adequate α/D leads to high search quality. But if we flip a small number of bits, HyperOMS cannot clearly differentiate the peak position. Also, since the peak shifts due to PTMs are not significant, spatial locality for a limited range is required. In the rest of our evaluation, we use $\alpha = D/2$, which shows the highest performance in most cases.

Encoding strategy. We compare the search quality of HyperOMS with the different binary encoding strategies. As discussed in Section 3.3, LSH [19, 26, 34], ID-Level HDC encoding [18, 25, 37] can be used alternatively to map raw data to binary vectors. Figure 5(c) compares the search quality of HyperOMS with the (1) proposed encoding method, (2) ID-Level HDC encoding that can capture the position of feature and its value, and (3) random projection-based LSH approach. Our encoding offers the best search quality compared to baselines.

Quantization level. High quantization levels may not be flexible to the peak intensity changes due to noise and PTMs. Low Q leads to low resolution in intensity capturing of the encoder. The quantization level Q did not significantly affect the search quality unless it falls in [8, 32]. Therefore, we use $Q = 16$.

4.3 Search Quality

We searched the iPRG2012 dataset against the yeast spectral library. As no ground truth information is available when analyzing complex biological data, instead, we compare our search quality with a list of consensus identifications produced by multiple search tools during the iPRG2012 study [10]. Figure 5(d) shows the search result of baseline tools. Among 7841 identifications in the iPRG2012 consensus result, HyperOMS is able to correctly identify 4141 spectra (Figure 5(b)). SpectraST and ANN-SoLo manage to identify 3891 and 5327 identifications, respectively.

We compared the performance of HyperOMS with the results from existing tools, including SpectraST and ANN-SoLo using the large-scale dataset. We used similar configurations for all tools, listed in Table 1. Figure 6 shows the number of identifications from the different search tools.

HyperOMS offers a higher search quality than SpectraST, i.e., HyperOMS identifies more spectra. ANN-SoLo managed to identify more spectra than our HyperOMS. Nevertheless, as described in

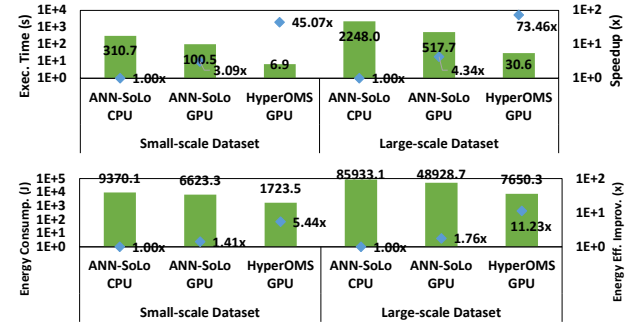


Figure 7: Performance and energy efficiency comparison.

Figure 6(b), HyperOMS can identify spectra that other tools can find (overlapped area). HyperOMS represents spectra with an approximated form of the original data, which is robust to PTMs. Therefore, HyperOMS can use Hamming similarity to perform OMS. Besides, ANN-SoLo uses shifted cosine similarity metric, which is accurate when finding the original spectra.

The identification rate of HyperOMS can be improved by increasing the HV capacity. This can be done by (1) increasing D or (2) increasing the precision of each component in the HV. For example, increasing D from 8k (8192) to 16k (16384) can yield up to 10% more identifications. However, it raises the hardware cost, computational complexity, and energy consumption of the accelerator. Since our main goal is to maximize the speed and energy efficiency of the OMS while achieving reasonable quality in a biological sense, we use a binary HV with 8k dimensionality.

A ramification of lower search quality could be missing potentially relevant biomarker proteins in the context of a healthy versus diseased study, or missing data similarly impacting other downstream biological interpretations. Nevertheless, the HyperOMS identification rate is within the range of the state-of-the-art in MS identification. For example, we can typically expect an identification rate of 33–66% currently for human samples that we have used, and HyperOMS satisfies the expected range criterion. One advantage of HyperOMS is that there is a search quality–efficiency trade-off that can be tuned using the hyperparameters. Furthermore, the user can decide between different search engines based on their requirements. For example, HyperOMS runs much faster with superior energy efficiency compared to existing OMS tools (Section 4.4). It could be used to efficiently process extremely large proteomics datasets consisting of tens of thousands of query files, which are being generated increasingly often recently.

4.4 Speed and Energy Efficiency Improvement

We compare the execution time and the energy consumption of HyperOMS on GPU to the state-of-the-art OMS tool ANN-SoLo, which offers a faster search speed with the GPU acceleration than other baseline [9]. Note that we measured the second run of the ANN-SoLo since the reference data is likely to be pre-encoded in reality. ANN-SoLo saves the pre-indexed information of the reference library on the first run and reuses it in the subsequent run. For the large-scale dataset, we averaged the measurements from multiple queries (b1906 ~ b1938).

Figure 7 compares the end-to-end runtime. ANN-SoLo builds the index on the CPU while the encoding of HyperOMS is done

on the GPU. The HyperOMS encoding is parallelized over HV dimensions and datapoints. The encoding stage of HyperOMS, which corresponds to the index build of ANN-SoLo, is up to $8.6\times$ faster than ANN-SoLo. HyperOMS uses HD binary vector and easily parallelizable Hamming similarity computation, while ANN-SoLo uses FP32 vector. The search process of HyperOMS GPU achieves on average $82\times$ speedup over ANN-SoLo on CPU and $11.2\times$ speedup ANN-SoLo on GPU. Ultimately, HyperOMS GPU offers significant speedup in all stages of the OMS. For the end-to-end execution, HyperOMS GPU gains an average speedup of $15.7\times$ over the state-of-the-art OMS tool running on the same GPU.

Besides, HyperOMS running on the GPU requires more power than the ANN-SoLo, as it has high parallelism. However, the increased power consumption is compensated by reduced execution time, improving energy efficiency. Overall, HyperOMS results in $7.8\times$ and $5\times$ energy efficiency improvement over CPU and GPU on average, respectively, as shown in Figure 7.

5 CONCLUSION

We proposed HyperOMS, HDC-inspired massively parallel algorithm for OMS of MS-based proteomics. The proposed algorithm encodes spectra into binary HVs, considering the spatial and value locality of peaks. Therefore, HyperOMS simplifies the execution pipeline and maximizes the computation efficiency and parallelism by using a binary vector with boolean operations. Our evaluation results show that HyperOMS offers comparable search quality to existing OMS tools. Furthermore, HyperOMS on NVIDIA Geforce GTX 1080Ti yields up to $17\times$ speedup and $6.4\times$ improved energy efficiency over the state-of-the-art GPU-based OMS solution.

ACKNOWLEDGMENTS

This work was supported in part by CRISP, one of six centers in JUMP (an SRC program sponsored by DARPA), SRC Global Research Collaboration (GRC) grant, and NSF grants #1826967, #1911095, #2052809, #2112665, #2112167, and #2100237.

REFERENCES

- [1] 2022. *MassIVE-KB*. <https://massive.ucsd.edu/ProteoSAFe/static/massive.jsp>
- [2] 2022. *MassIVE: Mass Spectrometry Interactive Virtual Environment*. <https://massive.ucsd.edu/>
- [3] C. Adams et al. 2022. Open modification searching of SARS-CoV-2-human protein interaction data reveals novel viral modification sites. (March 2022).
- [4] R. Aebersold et al. 2016. Mass-Spectrometric Exploration of Proteome Structure and Function. *Nature* 537, 7620 (Sept. 2016), 347–355.
- [5] A. A. Aksenov et al. 2017. Global chemical analysis of biology by mass spectrometry. *Nature Reviews Chemistry* 1, 7 (2017), 1–20.
- [6] L. A. Baumgardner et al. 2011. Fast Parallel Tandem Mass Spectral Library Searching Using GPU Hardware Acceleration. *J. Proteome Res.* 10, 6 (June 2011), 2882–2888.
- [7] W. Bittemieux et al. 2018. Fast Open Modification Spectral Library Searching through Approximate Nearest Neighbor Indexing. *J. Proteome Res.* 17, 10 (Sept. 2018), 3463–3474.
- [8] W. Bittemieux et al. 2018. Quality Control in Mass Spectrometry-Based Proteomics. *Mass Spectrom. Rev.* 37, 5 (Sept. 2018), 697–711.
- [9] W. Bittemieux et al. 2019. Extremely Fast and Accurate Open Modification Spectral Library Searching of High-Resolution Mass Spectra Using Feature Hashing and Graphics Processing Units. *J. Proteome Res.* 18, 10 (Aug. 2019), 3792–3799.
- [10] R. J Chalkley et al. 2014. Proteome Informatics Research Group (IPRG)_2012: A Study on Detecting Modified Peptides in a Complex Mixture. *MCP* 13, 1 (Jan. 2014), 360–371.
- [11] H. Chi et al. 2018. Comprehensive Identification of Peptides in Tandem Mass Spectra Using an Efficient Open Search Engine. *Nat. Biotechnol.* (Oct. 2018), <https://doi.org/10.1038/nbt.4236>
- [12] J. M Chick et al. 2015. A Mass-Tolerant Database Search Identifies a Large Proportion of Unassigned Spectra in Shotgun Proteomics as Modified Peptides. *Nat. Biotechnol.* 33, 7 (June 2015), 743–749.
- [13] A. Devabhaktuni et al. 2019. TagGraph Reveals Vast Protein Modification Landscapes from Large Tandem Mass Spectrometry Datasets. *Nat. Biotechnol.* 37, 4 (April 2019), 469–479.
- [14] Joshua E Elias et al. 2007. Target-Decoy Search Strategy for Increased Confidence in Large-Scale Protein Identifications by Mass Spectrometry. *Nature Methods* 4, 3 (Feb. 2007), 207–214.
- [15] A. A. Goloborodko et al. 2013. Pyteomics—a Python Framework for Exploratory Data Analysis and Rapid Software Prototyping in Proteomics. *J. Am. Soc. Mass Spectrom.* 24, 2 (Jan. 2013), 301–304.
- [16] J. Griss et al. 2013. PRIDE Cluster: Building a Consensus of Proteomics Data. *Nat. Methods* 10, 2 (Jan. 2013), 95–96.
- [17] M. Heck et al. 2020. Proteomics in Non-model Organisms: A New Analytical Frontier. *J. Proteome Res.* 19, 9 (2020), 3595–3606.
- [18] M. Imani et al. 2017. Voicehd: Hyperdimensional computing for efficient speech recognition. In *ICRC*.
- [19] M. Imani et al. 2020. DUAL: Acceleration of Clustering Algorithms using Digital-based Processing In-Memory. In *MICRO*.
- [20] J. Johnson et al. 2017. Billion-scale similarity search with GPUs. *arXiv preprint arXiv:1702.08734* (2017).
- [21] P. Kanerva. 2009. Hyperdimensional Computing: An Introduction to Computing in Distributed Representation with High-Dimensional Random Vectors. *Cognitive Computation* 1, 2 (Jan. 2009), 139–159.
- [22] J. Kang et al. 2022. OpenHD: A GPU-Powered Framework for Hyperdimensional Computing. *IEEE TC* (2022).
- [23] J. Kang et al. 2022. XCelHD: An Efficient GPU-Powered Hyperdimensional Computing with Parallelized Training. In *ASP-DAC*. 220–225.
- [24] Attila Kertesz-Farkas et al. 2015. Tandem Mass Spectrum Identification via Cascaded Search. *J. Proteome Res.* 14, 8 (Aug. 2015), 3027–3038.
- [25] Y. Kim et al. 2018. Efficient human activity recognition using hyperdimensional computing. In *IoT*. 1–6.
- [26] H. Koga et al. 2006. Fast agglomerative hierarchical clustering algorithm using Locality-Sensitive Hashing. *KAIS* 12, 1 (July 2006), 25–53.
- [27] A. T Kong et al. 2017. MSFragger: ultrafast and comprehensive peptide identification in mass spectrometry-based proteomics. *Nat. Methods* 14, 5 (April 2017), 513–520.
- [28] H. Lam. 2011. Building and searching tandem mass spectral libraries for peptide identification. *MCP* 10, 12 (2011).
- [29] H. Lam et al. 2007. Development and validation of a spectral library searching method for peptide identification from MS/MS. *PROTEOMICS* 7, 5 (March 2007), 655–667.
- [30] H. Lam et al. 2010. Artificial decoy spectral libraries for false discovery rate estimation in spectral library searching in proteomics. *J. Proteome Res.* 9, 1 (2010), 605–610.
- [31] Y. Li et al. 2014. Accelerating the scoring module of mass spectrometry-based peptide identification using GPUs. *BMC Bioinform.* 15, 1 (2014), 121.
- [32] C. W. M. Ma et al. 2014. Hunting for Unexpected Post-Translational Modifications by Spectral Library Searching with Tier-Wise Scoring. *J. Proteome Res.* 13, 5 (April 2014), 2262–2271. <https://doi.org/10.1021/pr01006g>
- [33] S. Na et al. 2015. Software Eyes for Protein Post-Translational Modifications. *Mass Spectrom. Rev.* 34, 2 (April 2015), 133–147.
- [34] M. Norouzi et al. 2012. Hamming Distance Metric Learning. In *NeurIPS*, Vol. 25.
- [35] Y. Perez-Riverol et al. 2022. The PRIDE database resources in 2022: a hub for mass spectrometry-based proteomics evidences. *Nucleic acids research* 50, D1 (2022).
- [36] P. Poduval et al. 2021. Robust In-Memory Computing with Hyperdimensional Stochastic Representation. In *NANOARCH*. 1–6.
- [37] S. Salamat et al. 2019. F5-hd: Fast flexible fpga-based framework for refreshing hyperdimensional computing. In *FPGA*. ACM, 53–62.
- [38] S. Salamat et al. 2020. Accelerating Hyperdimensional Computing on FPGAs by Exploiting Computational Reuse. *IEEE TC* 69, 8 (2020), 1159–1171.
- [39] N. Selevsek et al. 2015. Reproducible and Consistent Quantification of the *Saccharomyces cerevisiae* Proteome by SWATH-mass spectrometry. *MCP* 14, 3 (March 2015), 739–749.
- [40] R. Smith et al. 2014. Proteomics, Lipidomics, Metabolomics: A Mass Spectrometry Tutorial from a Computer Scientist’s Point of View. *BMC Bioinform.* 15, Suppl 7 (2014), S9.
- [41] C. T Walsh et al. 2005. Protein Posttranslational Modifications: The Chemistry of Proteome Diversifications. *Angew. Chem. Int. Ed.* 44, 45 (Nov. 2005), 7342–7372.
- [42] M. Wang et al. 2018. Assembling the Community-Scale Discoverable Human Proteome. *Cell Systems* 7, 4 (Oct. 2018), 412–421.e5.
- [43] M. Yang et al. 2019. A Complete CPU-FPGA Architecture for Protein Identification with Tandem Mass Spectrometry. In *ICFPT*. 295–298.
- [44] S. Zhang et al. 2021. Assessing Robustness of Hyperdimensional Computing Against Errors in Associative Memory. In *ASAP*. 211–217.